Published in final edited form as:

J Phys Chem B. 1999 September ; 103(36): 7613–7620. doi:10.1021/jp991469n.

Luminescence Spectral Properties of CdS Nanoparticles

Joseph R. Lakowicz, **Ignacy Gryczynski**, **Zygmunt Gryczynski**, **Catherine J. Murphy**[†]

University of Maryland School of Medicine, Center for Fluorescence Spectroscopy, Department of Biochemistry and Molecular Biology, 725 West Lombard Street Baltimore, Maryland 21201, and University of South Carolina, Department of Chemistry and Biochemistry, Columbia, South Carolina 29208

Abstract

We examined the steady state and time resolved luminescence spectral properties of two types of CdS nanoparticles. CdS nanoparticles formed in the presence of an amine-terminated dendrimer showed blue emission. The emission wavelength of these nanoparticles depended on the excitation wavelength. The CdS/dendrimer nanoparticles displayed polarized emission with the anisotropy rising progressively from 340 to 420 nm excitation, reaching a maximal value in excess of 0.3. To the best of our knowledge this is the first report of a constant positive polarized emission from luminescent nanoparticles. We also examined a second type of nanoparticle, polyphosphate-stabilized CdS. These polyphosphate-stabilized nanoparticles displayed a longer wavelength red emission maximum and displayed a zero anisotropy for all excitation wavelengths. Both nanoparticles displayed strongly heterogeneous intensity decays with mean decay times of 93 ns and 10 μs for the blue and red emitting particles, respectively. Both types of nanoparticles were found to be severalfold more photostable upon continuous illumination than fluorescein. Despite the long decay times, the nanoparticles are mostly insensitive to dissolved oxygen but were quenched by iodide. These results suggest that nanoparticles can provide a new class of luminophores for use in chemical sensing, DNA sequencing, high throughput screening and other biotechnology applications.

Introduction

There is presently widespread interest in the physical and optical properties of nanometer sized semiconductor particles, the so-called nanoparticles or quantum dots. It is known that the optical properties of such particles depend on their size.[1–6] Such particles display optical and physical properties which are intermediate between those of the bulk material and those of the isolated molecules. For example, the optical absorption of bulk CdSe typically extends to 690 nm. When CdSe is made into 40 Å nanoparticles the longest absorption band shifts to 530 nm.[1] In nanoparticles a large percentage of the atoms are in the surface, rather than in the bulk phase. Consequently, the chemical and physical properties of the material, such as the melting point or phase transition temperature, depend on the particle size. Nanoparticles can be made from a wide variety of materials including CdS, ZnS, Cd_3P_2, and PbS, to name a few. The nanoparticles frequently display photoluminescence and sometimes display

[†]University of South Carolina.

electroluminescence.[7–12] Additionally, some nanoparticles can form self-assembled arrays.[13–14] Because of those favorable properties, nanoparticles are being extensively studied for use in optoelectronic displays.

Photophysical studies of nanoparticles have been hindered by the lack of reproducible preparations of homogeneous size. The size of the particles frequently changes with time following preparation. This situation is now rapidly changing as a result of new methods in which the particle surface is coated with another semiconductor or other chemical species which stabilize the particles.[15–18]

The increasing availability of homogeneous sized nanoparticles suggests more detailed studies of their photophysical properties, which in turn could allow their use as biochemical probes. The first reports of such particles as cellular labels have just appeared.[19–20] CdS particles have also been synthesized which bind DNA and display spectral changes upon DNA binding.[21–23] In the present report we describe detailed studies of the steady state and time resolved emission of two types of stabilized CdS particles. CdS nanoparticles were fabricated in the presence of a starburst dendrimer.[24] These particles display blue emission. The second type of CdS particles were stabilized with polyphosphate[21] and display red emission.

Materials and Methods

Nanoparticle Preparation.

The blue emitting CdS particles were prepared in the presence of poly(aminoamine) starburst dendrimer, generation 4.0.[24] The starburst dendrimer (PAMAM) of generation 4.0 was purchased from Aldrich. This dendrimer is expected to have 64 surface amino groups and have a diameter near 40 Å. On the basis of the manufacturer's value of the dendrimer weight fractions in MeOH and the known dendrimer densities, we prepared dendrimer stock solutions of 1.14×10^{-4} M in MeOH under a N_2 atmosphere of 10 °C. The 2.0 mM stock solutions of Cd^{2+} and S^{2-} were prepared by dissolving 62 mg of $Cd(NO_3)_2 \cdot 4H_2O$ (Baker) in 100 mL of MeOH and by dissolving 15 mg Na_2S (Alfa) in 100 mL of MeOH. The Cd^{2+} and S^{2-} stock solutions were freshly prepared. In the standard incremental addition procedure, an 0.50 mL aliquot of Cd^{2+} stock solution was added to 10 mL of the dendrimer stock solution at 10 °C, followed by addition of an 0.50 mL aliquot of S^{2-}stock solution. The Cd^{2+} and S^{2-} additions were repeated 10 times. The resulting solution was colorless and glowed bright blue under UV illumination. The product was stored in a freezer and did not show any evidence of precipitation for months. The nature of this nanoparticle-dendrimer composite is not under-stood at this time, but the composite is stable for long periods of time in neutral methanol.

The red emitting particles are also composed of CdS, but stabilized with polyphosphate.[21] For the polyphosphate-stabilized (PPS) CdS nanoparticles, 2×10^{-4} $Cd(NO_3)_2 \cdot 4H_2O$ in degassed water was mixed with an equivalent amount of sodium polyphosphate, $Na_6(PO_3)_6$. Solid Na_2S was added, with vigorous stirring, to yield 2×10^{-4} M sulfide. The solution immediately turned yellow. Under UV light, the solution glowed red-orange.

Spectroscopic Measurements.

Frequency-domain (FD) intensity and anisotropy decays were measured with instrumentation described previously.[25] The excitation source was a HeCd laser at 325 or 442 nm. The continuous output of this laser was amplitude modulated with a Pockels' cell. The FD data were interpreted in terms of the multiexponential model

$$I(t) = \sum_i \alpha_i \exp(-t/\tau_i) \quad (1)$$

where α_i are the preexponential factors and τ_i the decay times. The fractional contribution of each decay time component to the steady state emission is given by

$$f_i = \sum_j \frac{\alpha_i \tau_i}{\alpha_j \tau_j} \quad (2)$$

Frequency-domain anisotropy decay data were measured and analyzed as described previously[26] in terms of multiple correlation times θk

$$r(t) = \sum_k r_{0k} \exp(-t/\theta_k) \quad (3)$$

In this expression r_{0k} is the fractional anisotropy amplitude which decays with a correlation time θ_k.

Results

While the absorption and emission spectra of nanoparticles have been widely studied, the scope of these measurements was typically limited to using the optical spectra to determine the average size of the particles. There have been relatively few studies of the time resolved photophysical properties of these particles. In the following sections we describe the steady state and time resolved emission of two types of CdS nanoparticles.

CdS/Dendrimer Nanocomposite.

Figure 1 shows the absorption and emission spectra of the CdS/dendrimer particles. One notices that there is a substantial Stokes' shift from 330 to 480 nm. Such a large Stokes' shift is a favorable property because the emission of the nanoparticles will be observable without homo energy transfer between the particles. Also, because of the substantial shift it should be relatively easy to eliminate scattered light from the detected signal by optical filtering.

The emission intensity of the blue nanoparticles is relatively strong. We estimated the relative quantum yield by comparing the fluorescence intensity with that of a fluorophore of known quantum yield, and an equivalent optical density at the excitation wavelength of 350 nm. As a quantum yield standard we used a solution of coumarin 1 in ethanol with a reported quantum yield of 0.73.[27] This comparison yields an apparent or a relative quantum yield of 0.097. We note that this value is not a molecular quantum yield because there is no consideration of the molar concentration of the nanoparticles. However, this value does indicate the relative brightness of the particles as compared to a known fluorophore. This

value is somewhat lower than reported previously,[24] which was a quantum yield near 0.17. At present we do not understand this discrepancy, but it is known to be difficult to accurately determine quantum yields. Also, it is possible that the quantum yields differ for different preparations of the nanoparticles.

For use as a luminescent probe the signal from the nanoparticles must be stable with continual illumination. In previous studies the emission intensities and/or emission spectra of nanoparticles have occasionally been found to depend on illumination.[28] In contrast, the CdS/dendrimer particles appear to be reasonably stable, about twofold more stable than fluorescein (Figure 2). We note that for these stability tests, the fluorescein and nanoparticles were illuminated with the focused output of a frequency-doubled Ti:sapphire laser. No changes in the emission intensity of the nanoparticles were found when illuminated with the output of a 450 W xenon lamp and monochromator.

CdS/Dendrimer Particles Display Polarized Emission.

For use as a biophysical probe of hydrodynamics a luminophore must display polarized emission. Since most nanoparticles are thought to be spherical, the emission is not expected to display any useful polarization. Importantly, the CdS/dendrimer particles were found to display high anisotropy (Figure 1). The anisotropy increases progressively as the excitation wavelength increases across the long wavelength side of the emission, from 350 to 430 nm. The emission anisotropy is relatively constant across the emission spectra. These properties, and the fact that the anisotropy does not exceed the usual limit of 0.4, suggest that the emission is due to a transition dipole similar to that found in excited organic molecules. The high and nonzero anisotropy also suggests that the excited state dipole is oriented in a fixed direction within the nanoparticles.

A fixed direction for the electronic transition suggests the presence of some molecular features which define a preferred direction for the transition moment. While most nanoparticles are thought to be spherical, the shape of the CdS inside of the CdS/dendrimer nanocomposite is not known. The electron micrographs[24] showed that the particles and dendrimers exist as larger aggregates rather than as isolated species. Unfortunately, the presence of aggregates prevented determination of the particle shape.[24] Our observation of a large nonzero anisotropy for these particles suggests an elongated shape for the quantum-confined state. To the best of our knowledge, this is the first observation of a constant positive polarized emission from CdS nanoparticles. The emission from silicon nanoparticles has been reported as unpolarized[29] or polarized.[30–32] Polarized emission has also been reported for CdSe.[33–34] However, in these cases the polarization is either negative or becomes negative in a manner suggesting a process occurring within the nanoparticle. Such behavior would not be useful for a fluorescence probe for which the polarization is expected to depend on rotational diffusion. The results in Figure 2 suggest that CdS/dendrimer nanoparticles can serve as hydrodynamic probes for rotational motions on the 50 to 400 ns time scale (see Figure 4 below). However, it is not yet known whether such a composite will be stable in a physiological environment which contains a variety of macromolecules. Also, methods to conjugate the dendrimer nanoparticles are not yet available. Such studies are needed prior to using these particles as biophysical probes.

Effect of Excitation Wavelength.

If the particle preparation has a single particle size, the emission spectra are expected to be independent of excitation wavelength. Hence we recorded the emission spectra for the CdS/dendrimer particles for a range of excitation wavelengths (Figure 3). Longer excitation wavelengths results in a progressive shift of the emission spectra to longer wavelengths. This effect is reminiscent of the well-known red edge excitation shift observed for organic fluorophores in polar solvents.[35–36] However, the molecular origin of the shift seen in Figure 3 is different. In this case, the shifts are probably due to the wavelength-dependent excitation of a selected subpopulation of the particles at each wavelength. In particular, longer excitation wavelengths probably result in excitation of larger particles with a longer wavelength emission maximum. Hence, this particular preparation of CdS/dendrimer particles appears to contain a range of particle sizes. However, we cannot presently exclude other explanations for the wavelength-dependent spectra seen in Figure 3.

Time Resolved Decay of the CdS/Dendrimer Particles.

We examined the time resolved intensity decay of the CdS/dendrimer particles using the frequency-domain method.[25–26] The frequency responses were found to be complex (Figure 4), indicating a number of widely spaced decay times. The FD data could not be fit to a single or double decay time model (Table 1). Three decay times were needed for a reasonable fit to the data, with decay times ranging from 3.1 to 170 ns. The mean decay time is near 117 ns. There seems to be a modest effect of excitation wavelength. The mean decay time decreases from 117 ns for excitation at 395 nm to 93 ns for excitation at 325 nm. Such long decay times are a valuable property for a luminescent probe, particularly one which can be used as an anisotropy probe. The long decay time allows the anisotropy to be sensitive to motions on a time scale comparable to the mean lifetime. Hence, one can imagine this particle being used as probes for the dynamics of large macromolecular structures, or even as model proteins since the nanoparticle size is comparable to the diameter of many proteins.

To better visualize the intensity decays, the parameters (α_i and τ_i) recovered from the least-squares analysis (Table 1) were used to reconstruct the time-dependent intensity decays (Figure5). The intensity is multi- or nonexponential at early times (insert) but does not display any long-lived microsecond components. While the intensity decay could be fit to three decay times, it is possible that the actual decay is more complex, and might be more accurately represented as a distribution of decay times.[37–39] Further experimentation is needed to clarify the nature of the intensity decay displayed by nanoparticles.

We also examined the frequency-domain anisotropy decay of the CdS/dendrimer particles (Figure 6). The differential polarized phase angles are rather low, with the largest phase angles centered near 1.0 MHz, suggesting rather long correlation times for the particles. Least-squares analysis of the FD anisotropy data revealed a correlation time near 2.4 μs (Table 1). Such a long correlation time is consistent with the observation that the CdS particles are aggregated with the dendrimers, or somehow present in a composite structure. Much shorter correlation time would be expected for particles with a size consistent with the optical properties, that is near 20 Å. We note that the time-zero anisotropy recovered from the FD anisotropy data is consistent with that expected from the excitation anisotropy

spectra and the excitation wavelength. This agreement suggests that the anisotropy of these particles decays because of overall rotational motion and not because of internal electronic properties of the particles. Hence, one can expect nanoparticles to be useful as analogues of proteins or other macromolecules and as internal cellular markers which could report the rate of rotational diffusion. Of course it would be necessary to prepare particles which are not aggregated.

Polyphosphate-Stabilized CdS Nanoparticles.

We also studied the spectral properties of a different type of CdS nanoparticle. These particles were stabilized with polyphosphate to the surface.[21] Absorption and emission spectra of these particles are shown in Figure 7. Compared to the CdS/dendrimer nanoparticles, these stabilized nanoparticles absorb and emit at much longer wavelengths. Their diameter was estimated to be 40 Å ± 15% by transmission electron microscopy. The spectra and intensities were found to be stable with prolonged illumination, at least fourfold more stable than fluorescein (Figure 2). The emission intensity of these red emitting particles is considerably weaker than the blue particles. The apparent quantum yield of the red particles was measured relative to DCM in methanol, with an assumed quantum yield of 0.38.[40] For equivalent optical densities at the excited wavelength of 442 nm, these particles display an apparent quantum yield of 0.015 and are thus less bright than the blue nanoparticle.

Compared to the blue emitting nanoparticles, these red emitting particles seem to display simpler and possibly less useful properties. The emission spectra were found to be independent of excitation wavelength, which suggest a highly homogeneous size distribution. The excitation spectrum (not shown) overlapped with the absorption spectrum. In an earlier preparation of such nanoparticles we noticed a long wavelength absorption above 480 nm which did not seem to be associated with any useful emission. This component did not appear in a later preparation. The absorption and excitation spectra of the CdS/dendrimer particles also appeared to be identical (Figure 1).

We examined the excitation and emission anisotropy spectra of these polyphosphate-stabilized particles. The anisotropy was found to be zero for all excitation and emission wavelengths. The zero anisotropy values could be due to rotational diffusion of the particles during the long luminescence decay (below). However, we could not detect any time-dependent decay of the anisotropy, as seen from the frequency-domain anisotropy data. We then examined the particles in 80% glycerol at −60 °C, and again found the anisotropies to be zero for excitation from 350 to 475 nm (Figure 8). Hence, it appears that these particles do not display any useful anisotropy. These results suggest that polarized emission is not a general property of nanoparticles, but requires special conditions of synthesis or stabilizers.

We examined the frequency-domain intensity decay of the stabilized nanoparticles (Figure 9). The intensity decay is complex, again requiring at least three decay times to fit the data (Table 2). The intensity decay in the time domain is shown in Figure 5. The decay times range from 150 ns to 25.3 μs, with a mean decay time near 9 μs. Once again there was an effect of excitation wavelength, but less than seen with the blue emitting nanoparticles.

Observation of microsecond decay times for these red emitting particles is an important result. There is currently considerable interest in using red or near-infrared (NIR) probes for noninvasive and/or in-vivo measurements.[41–43] Most such probes display relatively short decay times, typically less than 1 ns. While a few metal-ligand complexes are known to emit in the red and to display long lifetimes,[44] the choice of probes with long lifetimes is limited. These intensity decay data for the polyphosphate-stabilized nanoparticles suggest that such nanoparticle probes can provide a new class of luminophores with both long wavelength emission and long decay times.

Quenching of the CdS Nanoparticles.

We examined the effect of commonly used quenchers on the nanoparticle emission. The effect of oxygen is shown in Figure 10. Dissolved oxygen had a modest effect on the intensity from the CdS/dendrimer particles, with the emission being quenched by about 40% for equilibration at one atmosphere of oxygen (top). Remarkably, dissolved oxygen had no effect on the emission from the CdS-PPS particles (lower panel). This is particularly surprising given the long intensity decay time of these particles. Lack of oxygen quenching of a colloidal cadmium sulfide preparation was reported previously,[45] but without the decay time data one cannot judge the sensitivity to quenching shown by this colloid. The absence of quenching by oxygen could be a valuable result. For instance, the absence of oxygen quenching is a valuable property of the lanthanides, allowing long decay times in samples exposed to air. These results suggest that some nanoparticles may be insensitive to oxygen, and thus useful for high sensitivity gated detection as is used in the lanthanide-based immunoassays.

We also examined the effects of the collisional quenchers acrylamide and iodide on the nanoparticles. The CdS/dendrimer nanoparticles were quenched by both iodide and acrylamide (Figure 11, top). The CdS-PPS particles were quenched by iodide but not significantly by acrylamide (bottom). The quenching observed for both types of nanoparticles seems to be at least partially dynamic, as seen by the decrease in mean decay time (Figure 12 and Table 3). Previous studies have shown that the emission of porous silicon is affected by solvents[46–48] and that the emission of cadmium colloids was enhanced by alkylamines.[49] Additional research is needed to determine the mechanism responsible for the quenching of nanoparticle luminescence.

Discussion

What are the potential applications of nanoparticles as luminescent probes? As mentioned previously, nanoparticles may provide an approach to obtain red NIR emitting probes with long decay times, which are presently not available. Some long-decay-time phosphorescent porphyrins are known,[50–51] but such probes are readily quenched by oxygen. In contrast, we did not observe a significant effect of oxygen on the emission intensity the red nanoparticles. Hence, at least some nanoparticles appear to be resistant to quenching by oxygen, but it is not yet known if this is a general property of nanoparticles.

A favorable property of the nanoparticles is the long intensity decay time. This allows nanoparticles which display anisotropy to be used in hydrodynamic probes on the time

scales ranging from hundreds of nanoseconds to microseconds. This is a time scale not usually available to fluorescence without the use of specialized luminophores. At present, additional work is needed to understand how the luminescence decay times can be adjusted by changes in nanoparticles composition.

It is also important too determine if the emission from nanoparticles can be quenched by other dissolved or adsorbed quenchers. If so, what mechanisms of quenching are effective? Also, it seems possible that nanoparticles could display resonance energy transfer, as has been suggested in some early reports.[42–43] Energy transfer between nanoparticles has been detected.[52–53] Methyl viologen was reported to quench ZnS particle emission, but it is not known if the mechanism involved Förster transfer.[53] However, it is not known if the nanoparticles will display resonance energy transfer to absorbing dyes, or if nanoparticles display Förster transfer. Also, what are the transfer rates and distances, and is the transfer sensitive to an orientation factor?

Additionally, considerable development is required before these nanoparticles can be used as biophysical probes. Methods must be developed for conjugating them to macromolecules. In the case of the CdS/dendrimer, the particles are actually nanocomposites of unknown overall structure.[24] It is not known if the favorable anisotropy properties of these particles will be retained following conjugation.

And finally, it is important to determine whether nanoparticles can be fabricated as chemical sensors. Can the nanoparticle emission be sensitive to important species such as Ca^{2+}, pH, or chloride? Will attachment of analyte-dependent absorbers to the nanoparticles result in analyte-dependent emission? In summary, nanoparticles offer many possible opportunities for use as biochemical probes and sensors. Further studies are needed to determine the ranges of application possible with nanoparticle technology.

Acknowledgment.

This work was supported by the NIH, National Center for Research Resources (RR-08119), and by the National Science Foundation.

References and Notes

(1). Bawendi MG; Steigerwald ML; Brus LE The quantum mechanics of larger semiconductors clusters (“quantum dots”), Annu. Rev. Phys. Chem 1990, 41, 477–496.

(2). Martin CR; Mitchell DT Nanomaterials In, Anal. Chem. News Features 1998, 322A–327A.

(3). Weller H Colloidal semiconductor Q-particles: Chemistry in the transition region between solid state and molecules, Angew. Chem., Int. Ed. Engl 1993, 32, 41–53.

(4). Norris DJ; Bawendi MG; Brus LE Optical properties of semiconductor nanocrystals (quantum dots), Molecular Electronics (Jortner J, Ratner M, Eds.; Blackwell: Oxford, U.K., 1997, pp 281–323.

(5). Alivisatos AP Perspectives on the physical chemistry of semiconductor nanocrystals, J. Phys. Chem 1996, 100, 13226–13239.

(6). Alivisatos AP Semiconductor clusters, nanocrystals and quantum dots, Science 1996, 271, 933–937.

(7). Dabbousi BO; Bawendi MG; Onitsuka O; Rubner MF Electroluminescence from CdSe quantum-dot/polymer composites, Appl. Phys. Lett 1995, 66 (11), 1316–1318.

(8). Colvin VL; Schlamp MC; Alivisatos AP Light-emitting diodes made from cadmium selenide nanocrystals and a semiconducting polymer, Nature 1994, 370, 354–357.

(9). Zhang L; Coffer JL Electrochemiluminescence from calixarene-coated porous Si liquid junction cells, J. Phys. Chem. B 1997, 101 (35), 6874–6878.

(10). Artemyev MV; Sperling V; Woggon U Electroluminescence in thin solid films of closely packed CdS nanocrystals, J. Appl. Phys 1997, 81 (10), 6975–6977.

(11). Huang J; Yang Y; Xue S; Yang B; Liu S; Shen J Photoluminescence and electroluminescence of ZnS: Cu nanocrystals in polymeric networks, Appl. Phys. Lett 1997, 70 (18), 2335–2337.

(12). Artemyev MV; Sperling V; Woggon U Electroluminescence in thin solid films of closely packed CdS nanocrystals, J. Cryst. Growth 1998, 184/185, 374–376.

(13). Shen MY; Goto T; Kurtz E; Zhu; Yao, T. Photoluminescence properties of single CdSe quantum dots in ZnSe obtained in self-organized growth, J. Phys.: Condens. Matter 1998, 10, L171–L176.

(14). Zhang BP; Yasuda T; Wang WX; Segawa Y; Edamatsu K; Itoh T; Yaguchi H; Onabe K A new approach to ZnCdSe quantum dots, Mater. Sci. and Eng 1998, B51, 127–131.

(15). Eychmüller A; Mews A; Weller H A quantum dot quantum well: CdS/HgS/CdS, Chem. Phys. Lett 1993, 208 (1, 2), 59–62.

(16). Correa-Duarte MA; Giersig M; Liz-Marzàn LM Stabilization of CdS semiconductor nanoparticles against photodegradation by a silica coating procedure, Chem. Phys. Lett 1998, 286, 497–501.

(17). Hines MA; Guyot-Sionnest P Synthesis and characterization of strongly luminescing ZnS-capped CdSe nanocrystals, J. Phys. Chem 1996, 100, 468–471.

(18). Sooklal K; Cullum BS; Angel SM; Murphy CJ Photophysical properties of ZnS nanoclusters with spatially localized Mn^{2+}, J. Phys. Chem 1996, 100, 4551–4555.

(19). Bruchez M; Moronne M; Gin P; Weiss S; Alivisatos AP Semiconductor nanocrystals as fluorescent biological labels, Science 1998, 281, 2013–2016. [PubMed: 9748157]

(20). Chan WCW; Nie S Quantum dot bioconjugates for ultrasensitive nonisotropic detection, Science 1998, 281, 2016–2018. [PubMed: 9748158]

(21). Mahtab R; Rogers JP; Murphy CJ Protein-sized quantum dot luminescence can distinguish between “straight”, “bent,” and “kinked” oligonucleotides, J. Am. Chem. Soc 1995, 117, 9099–9100.

(22). Mahtab R; Rogers JP; Singleton CP; Murphy CJ Preferential adsorption of a “kinked” DNA to a neutral curved surface: Comparisons to and implications for nonspecific DNA-protein interactions, J. Am. Chem. Soc 1996, 118, 7028–7032.

(23). Murphy CJ; Brauns EB; Gearheart L Quantum dots as inorganic DNA-binding proteins, Proc. Materials Res. Soc 1997, 452, 597–600.

(24). Sookal K; Hanus LH; Ploehn HJ; Murphy CJ A blue-emitting CdS/dendrimer nanocomposite, Adv. Mater, 1998, 10, 1083–1087.

(25). Lakowicz JR; Gryczynski I Frequency-domain fluorescence spectroscopy. In Topics in Fluorescence Spectroscopy, Vol. 1: Topics in Fluorescence Spectroscopy; Lakowicz JR, Ed.; Plenum Press: New York, 1991; pp 293–355.

(26). Lakowicz JR; Cherek H; Kuśba J; Gryczynski I; Johnson ML Review of fluorescence anisotropy decay analysis by frequency-domain fluorescence spectroscopy, J. Fluoresc 1993, 3, 103–116. [PubMed: 24234774]

(27). Jones G; Jackson WR; Choi C-Y; Bergmark WR Solvent effects on emission yield and lifetime for coumarin laser dyes. Requirements for a rotatory decay mechanism, J. Phys. Chem 1985, 89, 294–300.

(28). Bahnemann DW; Kormann C; Hoffmann MR Preparation and characterization of quantum size zinc oxide: A detailed spectroscopic study, J. Phys. Chem 1987, 91, 3789–3799.

(29). Brus LE; Szajowski PF; Wilson WL; Harris TD; Schuppler S; Citrin PH Electronic spectroscopy and photophysics of Si nanocrystals: Relationship to bulk c-Si and porous Si, J. Am. Chem. Soc 1995, 117, 2915–2922.

(30). Andrianov AV; Kovalev DI; Zinov’ev NN; Yaroshetskil ID Anomalous photoluminescence polarization of porous silicon, JETP Lett. 1993, 58, 427–430.

(31). Kovalev D; Ben-Chorin M; Diener J; Averboukh B; Polisski G; Koch F Symmetry of the electronic states of Si nanocrystals: An experimental study, Phys. ReV. Lett 1997, 79 (1), 119–122.

(32). Koch F; Kovalev D; Averboukh B; Polisski G; Ben-Chorin M Polarization phenomena in the optical properties of porous silicon, J. Luminesc 1996, 70, 320–332.

(33). Chamarro M; Gourdon C; Lavallard P; Ekimov AI Enhancement of exciton exchange interaction by quantum confinement in CdSe nanocrystals, Jpn. J. Appl. Phys 1995, 34, 12–14.

(34). Bawendi MG; Carroll PJ; Wilson WL; Brus LE Luminescence properties of CdSe quantum crystallites: Resonance between interior and surface localized states, J. Chem. Phys 1992, 96 (2), 946–954.

(35). Demchenko AP Ultraviolet Spectroscopy of Proteins, Springer-Verlag: New York, 1981; pp 158–172.

(36). Vix A; Lami H Protein fluorescence decay: Discrete components or distribution of lifetimes? Really no way out of the dilemma? Biophys. J 1995, 68, 1145–1151. [PubMed: 7756534]

(37). Alcala JR The effect of harmonic conformational trajectories on protein fluorescence and lifetime distributions, J. Chem. Phys 1994, 101, 4578–4584.

(38). Lakowicz JR; Cherek H; Gryczynski I; Joshi N; Johnson ML Analysis of fluorescence decay kinetics measured in the frequency-domain using distribution of decay times, Biophys. Chem 1987, 28, 35–50. [PubMed: 3689869]

(39). Siemiarczuk A; Wagner BD; Ware WR Comparison of the maximum entropy and exponential series methods for the recovery of distribution of lifetimes from fluorescence lifetime data, J. Phys. Chem 1990, 94, 1661–1666.

(40). Gryczynski I; Kuśba J; Lakowicz JR Effects of light quenching on the emission spectra and intensity decays of fluorophore mixtures, J. Fluoresc 1997, 7 (3), 167–183. [PubMed: 32189960]

(41). Thompson RB Red and near-infrared fluorometry In Topics in Fluorescence Spectroscopy, Vol. 4: Design Probe and Chemical Sensing; Lakowicz JR, Ed.; Plenum Press: New York, 1994; pp 151–181.

(42). Casay GA; Shealy DB; Patonay G Near-infrared fluorescence probes In Topics in Fluorescence Spectroscopy, Vol. 4: Design Probe and Chemical Sensing; Lakowicz JR, Ed.; Plenum Press: New York, 1994; pp 183–222.

(43). Daehne S; Resch-Genger U; Wolfbeis OS, Eds. Near-infrared Dyes for High Technology Applications, Proceedings of the NATO Advanced Research Workshop on Syntheses, Optical Properties and Applications of Near-Infrared (NIR) Dyes in High Technology; Kluwer Academic Publishers: Czech Republic, 1998; p 468.

(44). Kober EM; Marshall JL; Dressick WJ; Sullivan BP; Caspar JV; Meyer TJ Synthetic control of excited states. Nonchro-mophoric ligand variations in polypyridyl complexes of osmium(II), Inorg. Chem 1985, 24, 2755–2763.

(45). Henglein A Photodegradation and fluorescence of colloidal-cadmium sulfide in aqueous solution, Ber. Bunsen. Phys. Chem 1982, 86, 301–305.

(46). Jin WJ; Shen GL; Yu RQ Organic solvent induced quenching of porous silicon photoluminescence, Spectrochim. Acta A 1998, 54, 1407–1414.

(47). Chun JKM; Bocarsly AB; Cottrell TR; Benziger JB; Yee JC Proton gated emission from porous silicon, J. Am. Chem. Soc 1993, 115, 3024–3025.

(48). Lauerhaas JM; Credo GM; Heinrich JL; Sailor MJ Reversible luminescence quenching of porous Si by solvents, J. Am. Chem. Soc 1992, 114, 1911–1912.

(49). Dannhauser T; O'Neil M; Johansson K; Whitten D; McLendon G Photophysics of quantized colloidal semiconductors dramatic luminescence enhancement by binding of simple amines, J. Phys. Chem 1986, 90, 6074–6076.

(50). Drain CM; Gentemann S; Roberts JA; Nelson NY; Medforth CJ; Jia S; Simpson MC; Smith KM; Fajer J; Shelnutt JA; Holten D Picosecond to microsecond photodynamics of a nonplanar nickel prophyrin: Solvent dielectric and temperature effects, J. Am. Chem. Soc 1998, 120, 3781–3791.

(51). Yusa S; Kamachi M; Morishima Y Photophysical behavior of Zinc(II) tetraphenylporphyrin covalently incorporated in a cholesterol bearing polymethacrylate, Photochem. Photobiol 1998, 67 (5), 519–525.

(52). Kagan CR; Murray CB; Nirmal M; Bawendi MG Electronic energy transfer in CdSe quantum dot solids, Phys. Rev. Lett 1996, 76 (9), 1517–1520. [PubMed: 10061743]

(53). Kagan CR; Murray CB; Bawendi MG Long-range resonance transfer of electronic excitations in close-packed CdSe quantum-dots solids, Phys. Rev. B 1996, 54 (12), 8633–8643.

(54). Weller H; Koch U; Gutierrez M; Henglein A Photochemistry of colloidal metal sulfies. 7. Absorption and fluorescence of extremely small ZnS particles (The World of the Neglected Dimensions), Ber. Bunsen-Ges. Phys. Chem 1984, 88, 649–656.

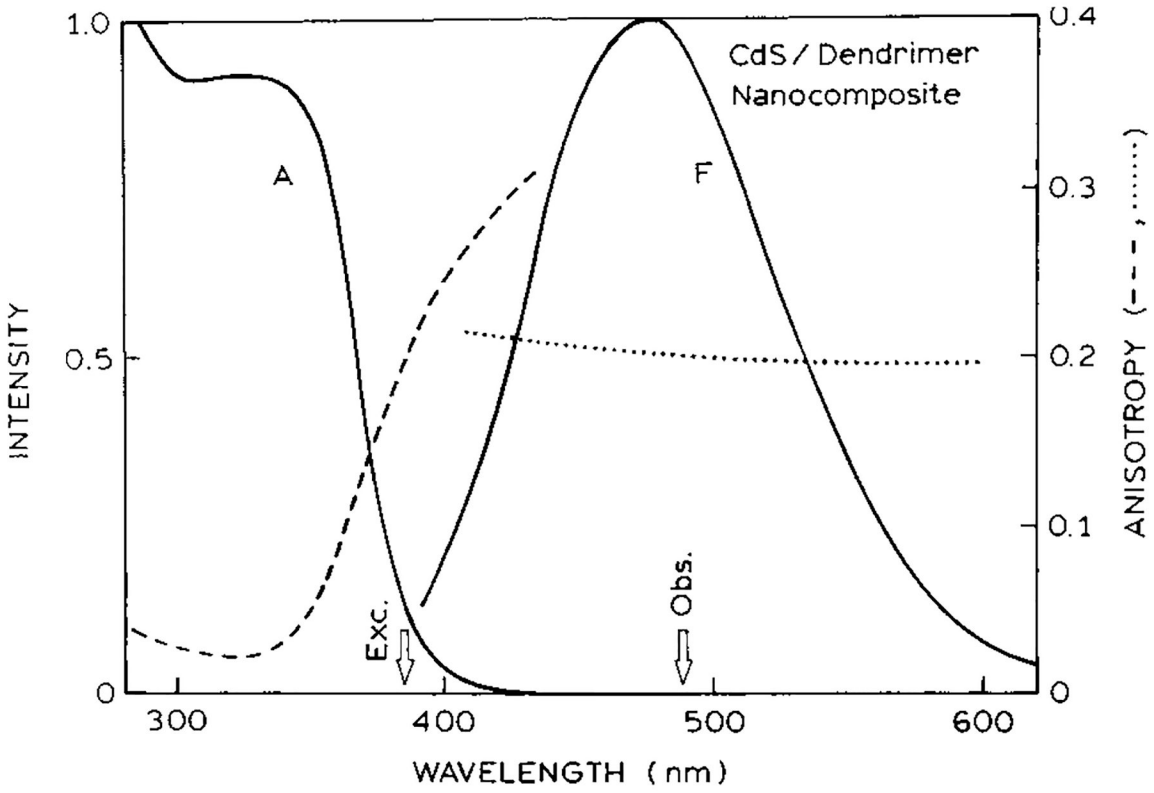

Figure 1.

Absorption and emission spectra of the blue emitting CdS/dendrimer nanocomposite in methanol at room temperature. The excitation spectrum of this nanoparticle overlaps with the absorption spectrum. Also shown are the excitation and emission anisotropy spectra, also in methanol at room temperature.

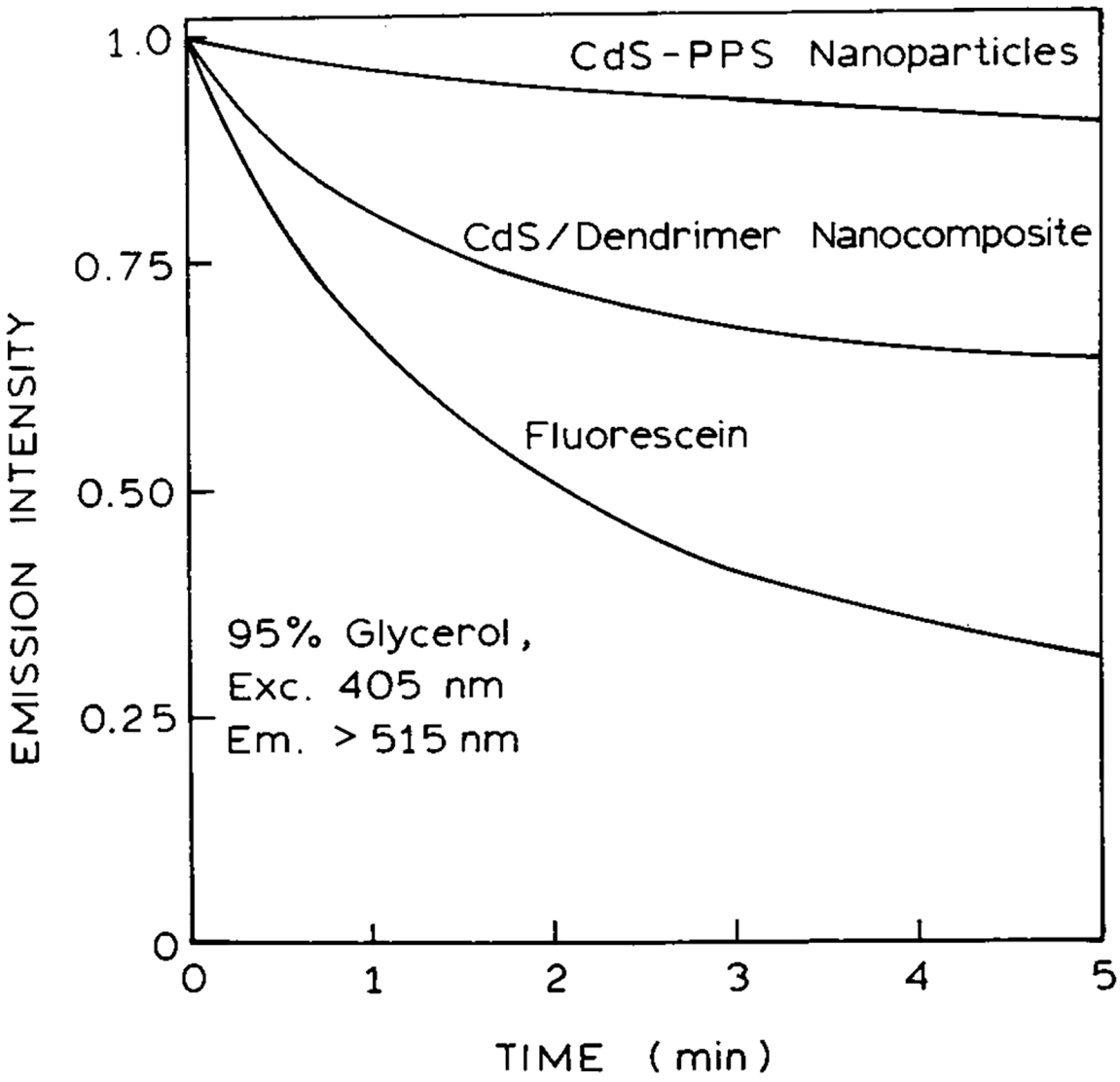

Figure 2.

Photostability tests of the CdS/dendrimer and polyphosphate-stabilized (PPS) nanoparticles. The sample was contained in a standard 1 cm × cm (4 mL) cuvette. The incident power was 30 mW at 405 nm from a frequency-doubled Ti:sapphire laser, 80 MHz, 200 fs, which was focused with a 2 cm focal length lens. Also shown is the intensity from fluorescein, pH 8, under comparable conditions. When illuminated with the output of a 450 W xenon lamp (385 nm for blue and 405 nm for red nanoparticles) there was no observable photobleaching.

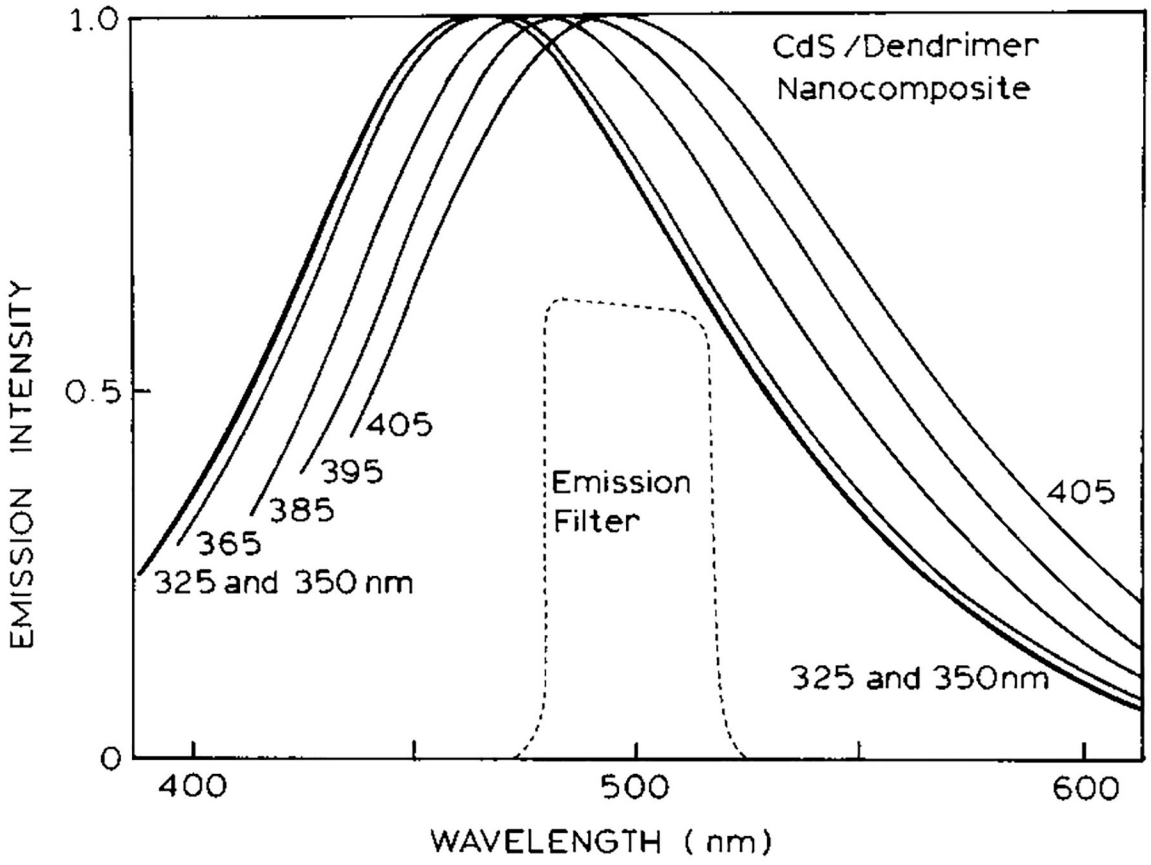

Figure 3.

Emission spectra of the CdS/dendrimer composite for different excitation wavelengths. Also shown as the dashed line is the transmission profile of the filter used for the time resolved measurements.

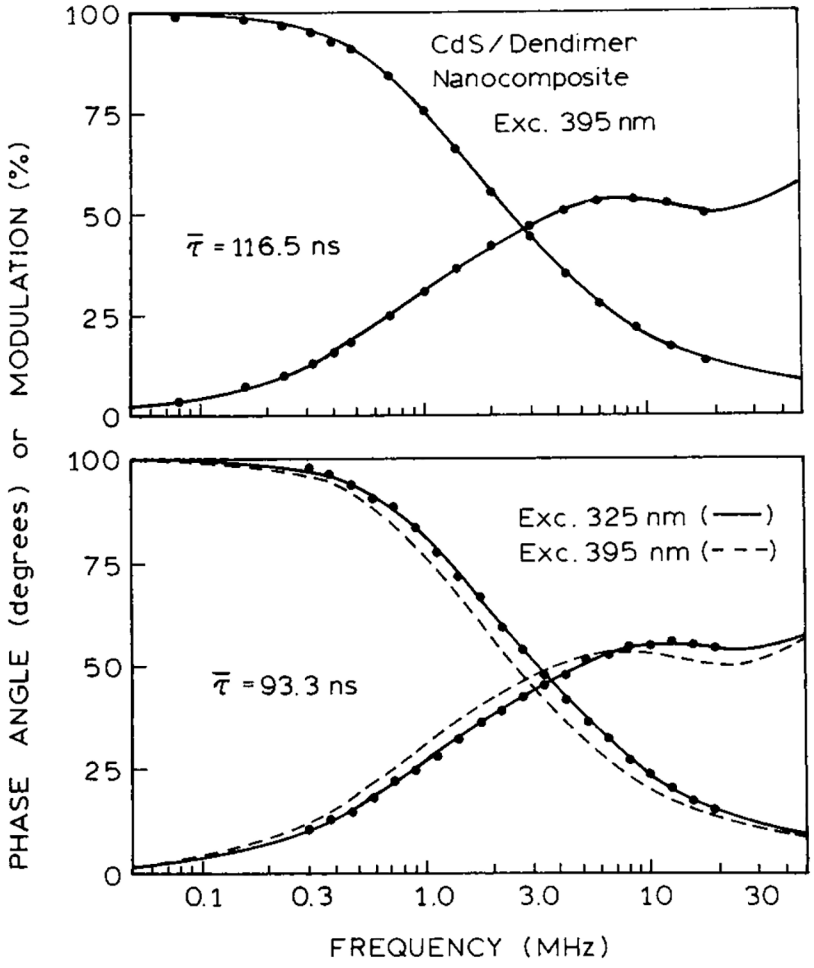

Figure 4.

Frequency-domain intensity decay of the CdS/dendrimer nanocomposite for excitation at 395 nm (top) and 325 nm (bottom). This solid line shows the best three decay time fits to the data.

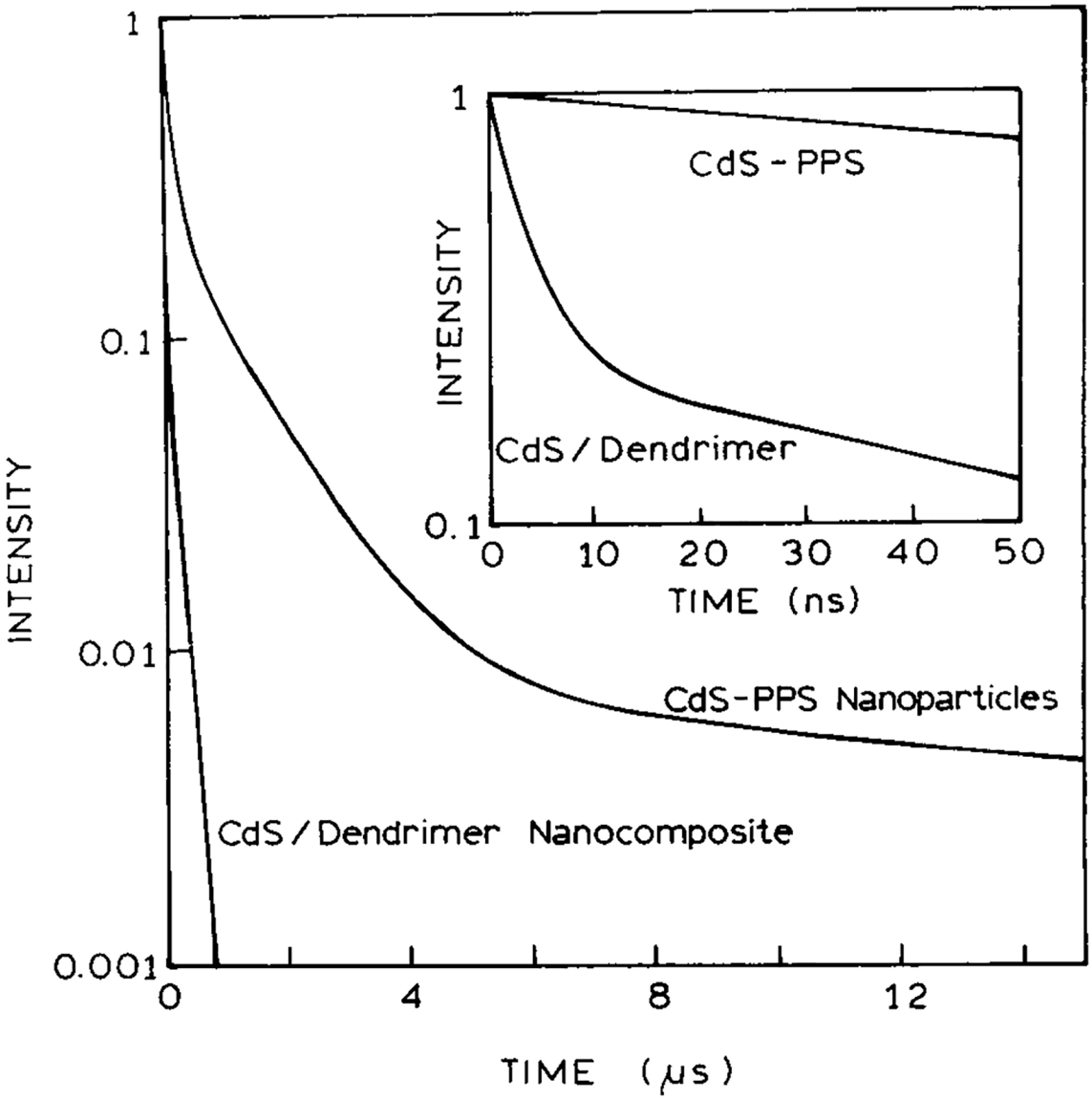

Figure 5.
Time-dependent intensity decays of the nanoparticles reconstructed from the frequency-domain data (Tables 1 and 2).

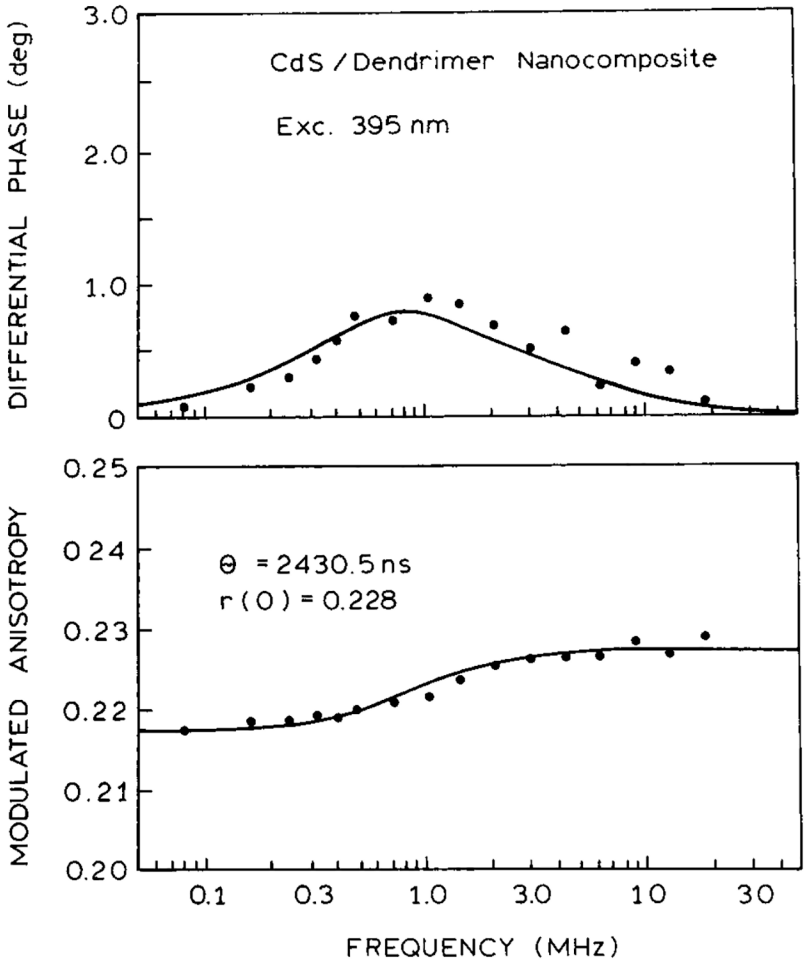

Figure 6.

Frequency-domain anisotropy decay of the CdS/dendrimer nanocomposite for excitation at 395 nm, at room temperature in methanol.

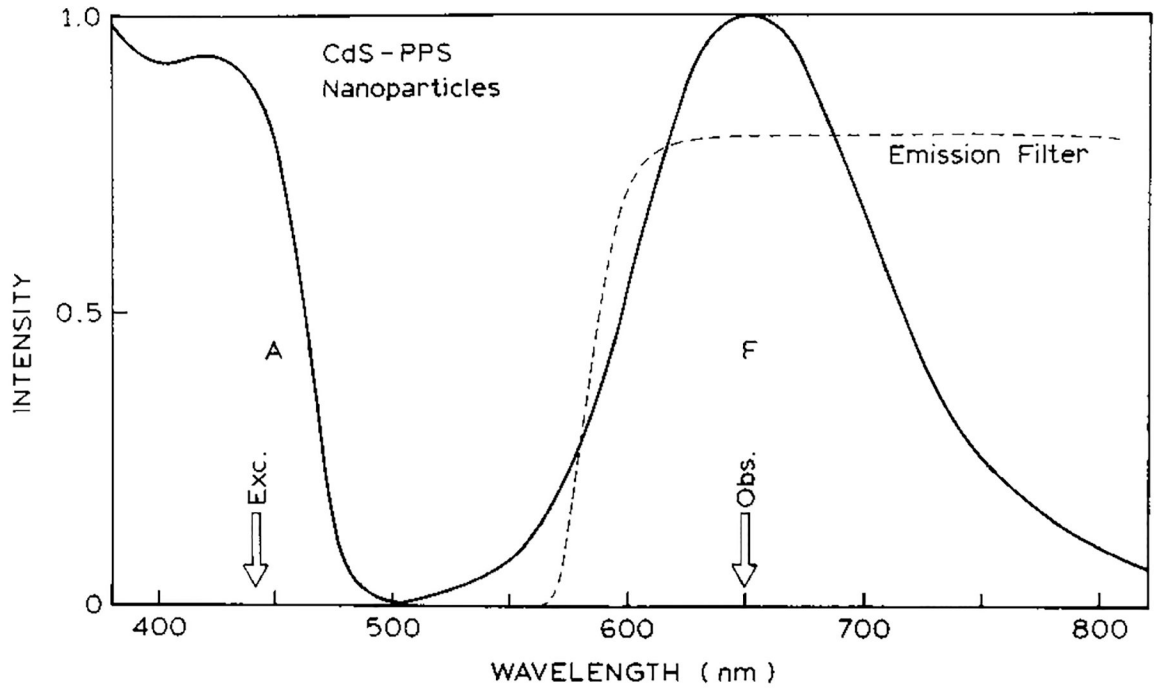

Figure 7.

Absorption (A) and emission (F) spectra of the CdS-PPS nanoparticles. In this case, the emission spectra were found to be independent of excitation wavelengths from 325 to 450 nm. The dashed line shows the transmission of the filter used to record the time resolved data.

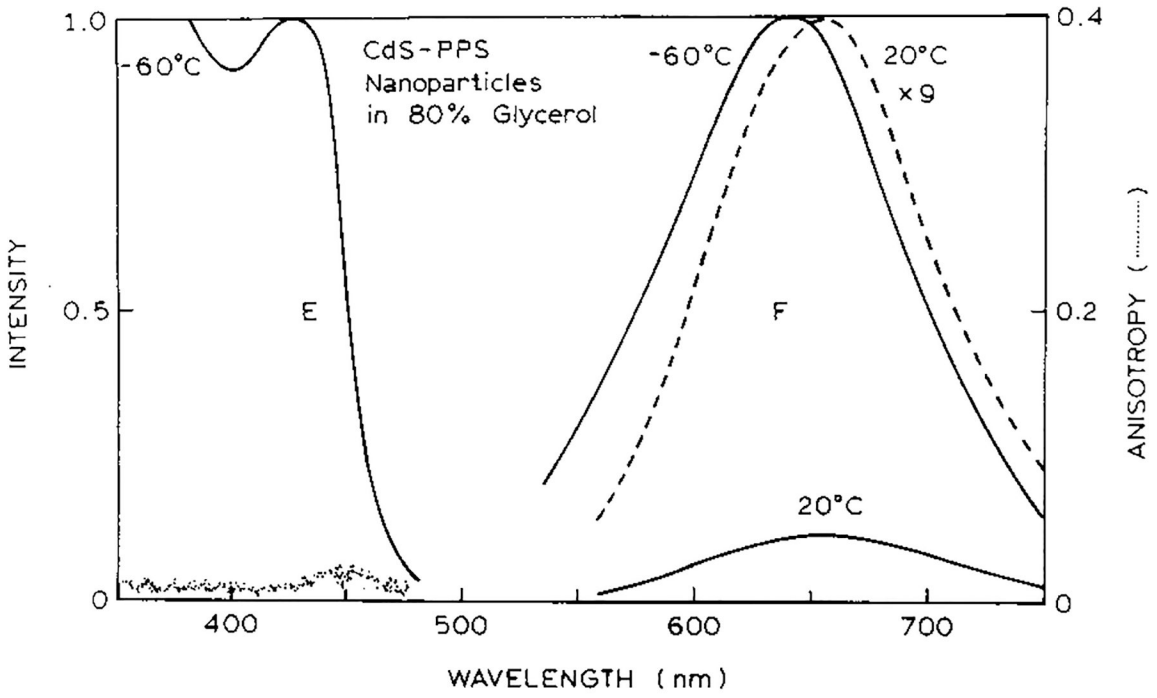

Figure 8.

Excitation anisotropy spectra of the CdS-PPS nanoparticles in 80% glycerol at −60 °C (dots). Also shown are the temperature-dependent spectra in 80% glycerol.

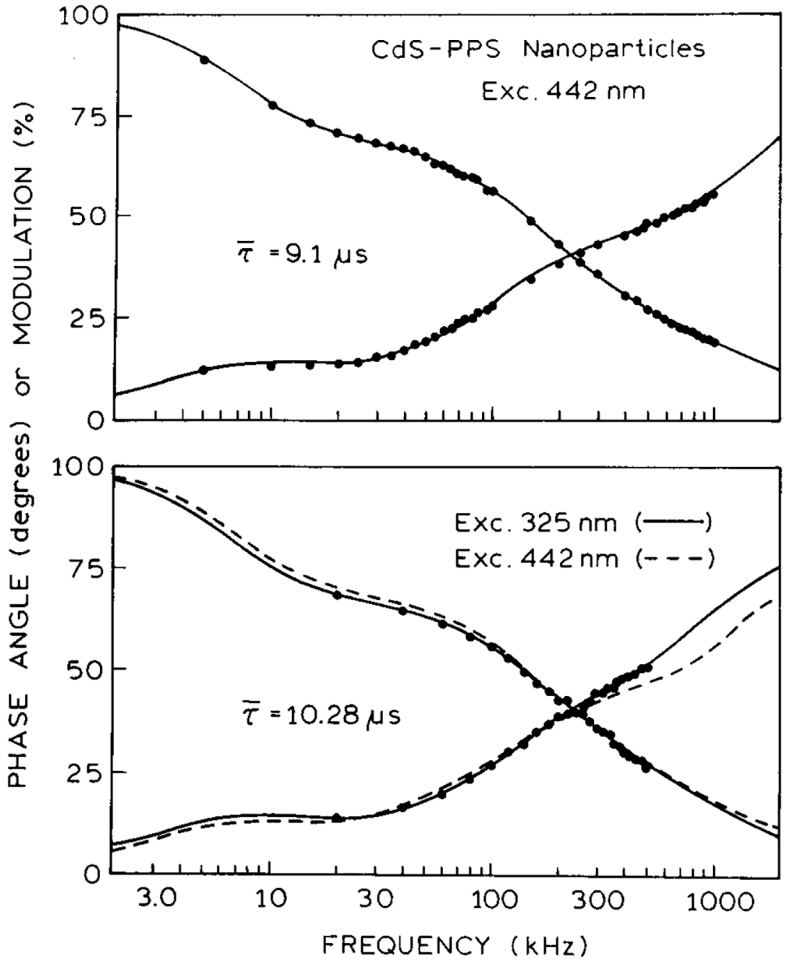

Figure 9.

Frequency-domain intensity decay of the CdS-PPS nanoparticles for excitation at 442 nm (top) and 325 nm (bottom). The solid lines show the best three decay time fits to the data.

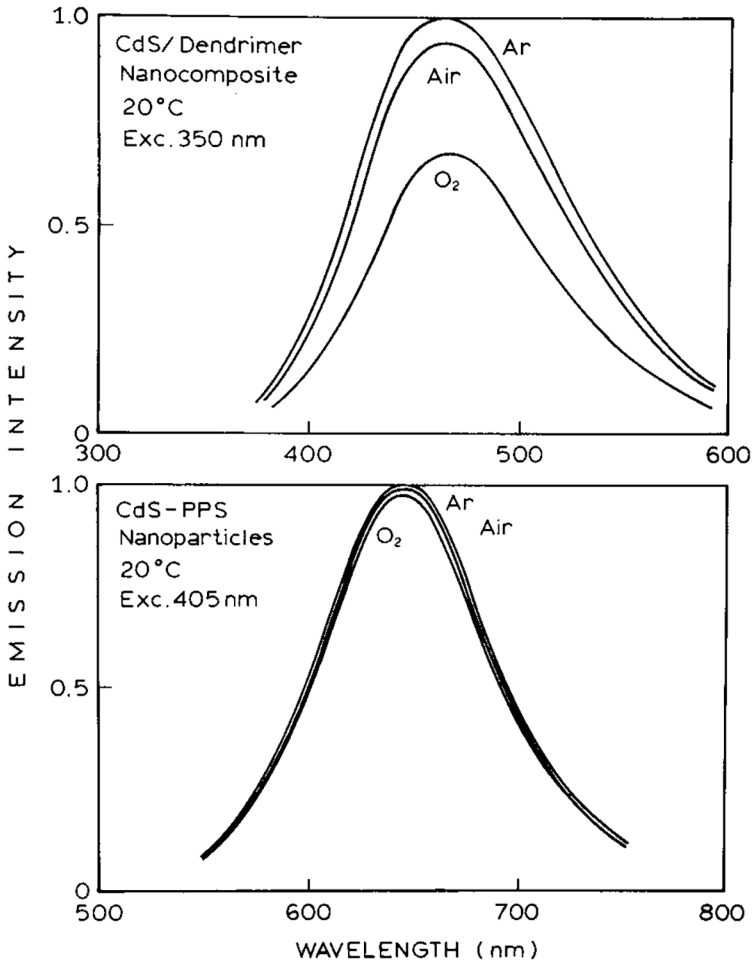

Figure 10.
Effect of oxygen on the emission spectra of the CdS/dendrimer and CdS-PPS nanoparticles.

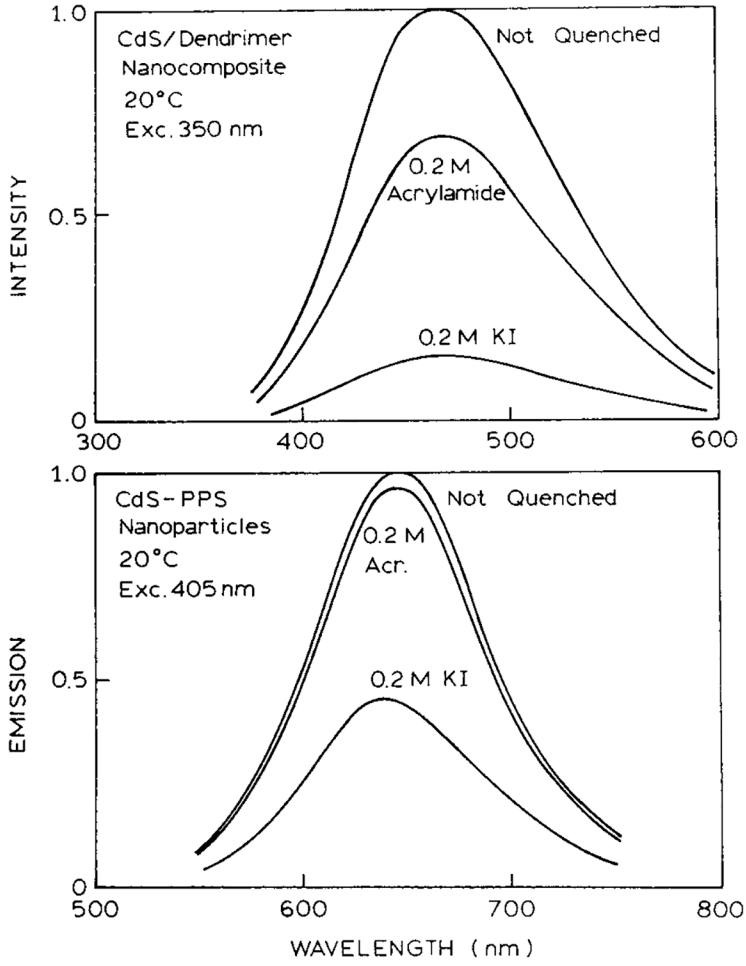

Figure 11.

Effect of acrylamide and iodide on the emission spectra of the CdS/dendrimer and CdS-PPS nanoparticles.

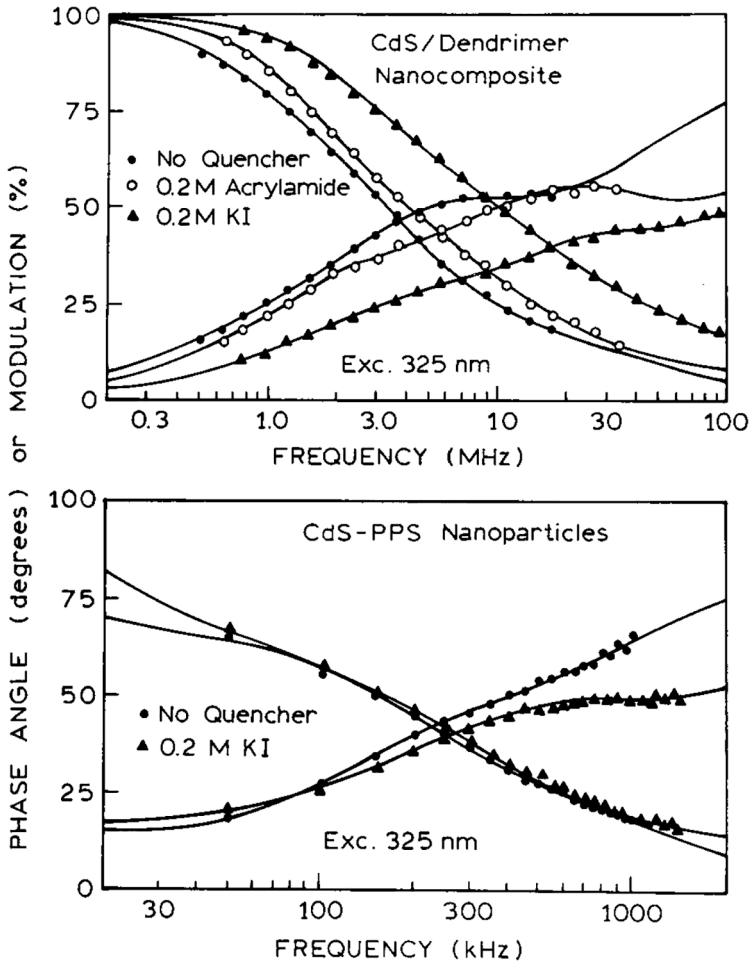

Figure 12.

Intensity decays of the CdS/dendrimer (top) and CdS-PPS nanoparticles (bottom) in the absence and presence of 0.2 M acrylamide or 0.2 M iodide. These measurements were done independently of those presented in Figures 4 and 9. For the CdS/dendrimer nanocomposite (top panel) the recovered average lifetimes ($\tau = 3f_i\tau_i$) are 106.0 ns for not quenched (●), 73.7 ns in the presence of 0.2 M acrylamide (○), and 36.7 ns in the presence of 0.2 M KI (▲). For the CdS-PPS nanoparticles (lower panel), average lifetimes are 9.80 μs for not quenched (●), 8.45 μs in the presence of 0.2 M acrylamide (not shown), and 4.09 μs in the presence 0.2 M KI (▲).

TABLE 1:

Frequency-Domain Intensity and Anisotropy Decays of the CdS/Dendrimer Nanoparticles

exc. (nm)	intensity decay					anisotropy decay			
	n^a	τ_i (ns)	α_i	f_i	X_R^2	n^a	θ_k (ns)	r_{0k}	χ_R^2
395	1	61.8	1.0	1.0	1,136.9	1	2430.5	0.228	0.6
	2	6.2	0.747	0.137					
		116.0	0.253	0.863	32.0				
	3	3.1	0.748	0.090					
		50.2	0.163	0.319					
		169.8	0.089	0.591	1.1				
325	1	52.3	1.0	1.0	991.5				
	2	7.8	0.705	0.160					
		97.9	0.295	0.890	37.5				
	3	2.7	0.699	0.080					
		39.5	0.205	0.341					
		142.8	0.096	0.579	1.7				

[a]Number of exponents.

TABLE 2:

Frequency-Domain Intensity Decay of the CdS-PPS Nanoparticles

		intensity decay			
exc. (nm)	**n**	**τ_i (ns)**	**α_i**	f_i	χ_R^2
442	1	597.5	1.0	1.0	1655.9
	2	290.4	0.932	0.448	
		4907.3	0.068	0.552	242.9
	3	150.0	0.749	0.188	
		1171.2	0.243	0.476	
		25320.0	0.008	0.336	2.7
325	1	680.2	1.0	1.0	1212.3
	2	425.0	0.932	0.474	
		6470.9	0.068	0.526	93.5
	3	241.6	0.717	0.227	
		1172.7	0.273	0.421	
		27783.0	0.010	0.352	2.9

[a]Number of exponents.

TABLE 3:

Intensity Decays of the Nanoparticles in Absence and Presence of Quenchers

compd/conditions[a]	$\bar{\tau}$ (ns)[b]	α_1	τ_1 (ns)	α_2	τ_2 (ns)	α_3	τ_3 (ns)	χ^2_R
blue, no quencher	106.0	0.698	4.91	0.256	57.7	0.046	214.2	2.2
+ 0.2 M acr.	73.7	0.737	1.07	0.190	18.0	0.073	105.9	4.2
+ 0.2 M KI	36.7	0.786	1.11	0.175	11.2	0.039	67.3	4.6
red, no quencher	9800	0.652	232.5	0.337	1073.3	0.011	25850	3.8
+ 0.2 M acr.	8540	0.761	229.3	0.229	1173.0	0.010	23490	1.9
+ 0.2 M acr.	4090	0.738	56.3	0.243	673.7	0.019	8582	3.2

[a]The excitation was 325 nm. The emission filter for the blue particles was an interference filter 500 “ 20 nm. For the red particles we used a long pass filter at 580 nm.

[b]$\bar{\tau} = \sum_i f_i \bar{\tau}_i,\ f_i = \alpha_i\tau_i / \sum \alpha_i\tau_i$.